A scanning probe and quartz crystal microbalance study of the impact of $C_{60}$ on friction at solid-liquid interfaces



2001 J. Phys.: Condens. Matter 13 4991

(http://iopscience.iop.org/0953-8984/13/21/323)

INSTITUTE OF PHYSICS PUBLISHING JOURNAL OF PHYSICS: CONDENSED MATTER

J. Phys.: Condens. Matter **13** (2001) 4991–4999 www.iop.org/Journals/cm PII: S0953-8984(01)20191-X

# A scanning probe and quartz crystal microbalance study of the impact of $C_{60}$ on friction at solid–liquid interfaces

**T Coffey, M Abdelmaksoud and J Krim**[1]

Physics Department, North Carolina State University, NC, USA

Received 18 December 2000

E-mail: jkrim@unity.ncsu.edu (J Krim)

**Abstract**

We have investigated the changes in interfacial friction of toluene on mica and Ag(111) both in the presence and in the absence of interfacial $C_{60}$ layers employing atomic force microscope (AFM) and quartz crystal microbalance (QCM) techniques. The lateral force measurements fail to detect $C_{60}$ at the toluene/mica interface, presumably because the $C_{60}$ is dislodged by the slow-moving probe tip. In contrast, QCM measurements of interfacial friction and slippage for toluene/Ag(111) are sensitive to the presence of interfacial $C_{60}$. We see the friction double when $C_{60}$ is present. The results are discussed in the light of the full-slip boundary condition which had been previously reported for surface forces apparatus (SFA) measurements on toluene/mica in the presence and absence of interfacial $C_{60}$.

## 1. Introduction

Introductory treatments of the topic of friction generally begin with Amonton's law for contacting solids:

$$F_f = \mu_s N \qquad F_f = \mu_k N \tag{1}$$

where $F_f$ is the force of friction, $\mu_s$ and $\mu_k$ are the coefficients of static and kinetic friction, respectively, and $N$ is the normal load. For solid–solid interfaces, the true area of contact is usually much smaller than the apparent area of contact, due to the presence of multi-asperity contact points. As the normal force increases, the number of contacting points increases, giving rise to Amonton's law. In contrast to the case for solid–solid contact, the true area of contact at a solid–liquid interface is the same as the apparent area of contact, irrespective of any externally applied forces. It should therefore be no surprise that a friction law associated with the solid–liquid geometry might not be described by Amonton's law. Indeed, for solid objects moving through a viscous retarding fluid, a retarding force of the form

$$F_f = \eta v \tag{2}$$

[1] Author to whom any correspondence should be addressed.

0953-8984/01/214991+09$30.00  

is frequently adequate, where $\eta$ is a coefficient of friction and $v$ is the relative solid–liquid velocity.

The field of nanotribology, or the study of friction and wear at submicron length scales, encompasses a number of experimental techniques involving single contact in both solid–solid and solid–liquid geometries. These techniques include probe-based methods such as atomic force microscopy (AFM), use of the surface forces apparatus (SFA), use of the quartz crystal microbalance (QCM) and the very recently developed 'blow-off experiment' [1]. For the QCM, the SFA, the blow-off experiment, and ideally for AFM, the true area of contact is equal to the apparent area of contact. Given the unique experimental geometries involved, the appropriate friction governing nanotribological behaviour is of current interest.

The AFM, SFA and QCM techniques have made important contributions to the understanding of nanotribology. The AFM was adapted for atomic-scale friction measurements in 1987 by Mate, McClelland, Erlandsson and Chang [2]. AFM observations by Mate *et al* [2] of a tungsten wire sliding on a basal plane of graphite were the first to directly link the structure of a surface with the dynamical frictional properties of an interface. A few years later, Germann *et al* [3] demonstrated frictional forces with no load dependence; this showed a departure from the classic Amonton law of macroscale friction. Nonetheless, most AFM measurements do in fact depend on the load, and obey Amonton's law. This implies a less-than-ideal tip which makes contact with the sample at multiple asperities. Germann *et al* avoided this problem by conducting their experiments in vacuum with a carefully constructed tip.

The SFA [4] has been used to study the dependence of the frictional force for a range of temperatures, adhesive strengths, sliding speeds and ambient environments [5]. Israelachvili and colleagues [6] used the SFA to study the friction between mica surfaces, and found friction to be proportional to the area of contact. Hirano *et al* employed the SFA to demonstrate that the friction between mica surfaces in a dry argon environment depended upon the commensurability of the surfaces in contact [7]. For SFA measurements, the frictional force is not generally linearly proportional to the applied load. However, both static and kinetic friction are observed in the sense that a yield stress (static friction) is required to initiate sliding (kinetic friction).

The QCM has been used for decades for micro-weighing purposes [8], and was adapted for friction measurements in 1986–88 by Widom and Krim [9–11]. Krim *et al*, employing a QCM, observed that solid krypton monolayers exhibited lower shear stresses than liquid krypton monolayers, and that sometimes interfaces are 'slippery when dry' [12]. QCMs were also used to demonstrate the electronic contribution to friction by showing the drop in friction upon achieving the superconducting state [13]. Static friction has never been evident in QCM measurements, with both solid–solid and liquid–solid interfaces being well described by the viscous friction law of equation (2).

Mate and Marchon have recently attempted to 'bridge the gap' between the QCM and SFA experimental geometries [1]. They focused on the fact that while both QCM and SFA measurements of the shearing of liquid films reveal viscous friction, static friction is present only in the SFA geometry. Mate and Marchon, employing a 'blow-off experiment', explored whether the open geometry or much greater shear rates of the QCM could account for the difference in the observed behaviours. Their results (which were obtained in an open geometry at very low shear rates) yielded viscous friction, showing that the differences between QCM and SFA results are due to their geometries.

By using the blow-off experiment as an intermediary technique, Mate and Marchon have taken a first step in cross-referencing the various nanotribological techniques. Nonetheless, interfaces composed of identical material have never been studied by even two out of the four experimental techniques. This is because the various nanotribological probes have very

different geometries and cover different ranges of shear stress, length scale, timescale and sliding speed, and lend themselves well to differing experimental systems. Studying the same interface with each technique to cross-reference the friction would provide an understanding of how these very different techniques relate to one another, and exactly how each technique measures friction. It would also enable better selection of the appropriate technique to use for studying any given system.

In order to mutually cross-reference the results of various nanotribological probes and to compare nanotribological results to macroscale ones, we have performed AFM and QCM investigations of the changes in interfacial friction and wetting of toluene on single-crystal substrates both in the presence and in the absence of $C_{60}$ adsorbed layers. We chose the system of $C_{60}$ in toluene on mica substrates to allow correlation of our results with those of Campbell *et al* [14] who employed the SFA to investigate $C_{60}$ dissolved in toluene on mica. They reported that the $C_{60}$ adsorbed as monolayers on the mica surfaces immersed in liquid toluene. These adsorbed layers, however, interacted very weakly with each other and with the mica surface. Due to their weak interactions, the adsorbed $C_{60}$ layers possessed unusually high fluidity, and they were easily pushed out of the way when the surfaces were brought slowly together. When the mica surfaces were sheared in the presence of the adsorbed layers, fluid flow between the two mica surfaces was reported to exhibit full-slip boundary conditions. For the pure toluene between the mica surfaces, the fluid exhibited a typical no-slip boundary condition. The $C_{60}$ adsorbed layers therefore produced '*an effective boundary of near-zero drag on the adjacent liquid*' [14].

Due to the round shape and the weak van der Waals interaction of $C_{60}$ molecules, there has been much speculation on the potential lubricating properties of fullerenes. The frictional properties of $C_{60}$ have therefore been widely investigated by a variety of techniques. In some studies, as a lubricant additive or for metal contacts, fullerenes and fullerene-like molecules have been shown to reduce friction [15–18]. Other AFM studies, however, have shown an increase in friction for surfaces with solid film coatings of $C_{60}$ [19, 20]. Most studies of $C_{60}$ molecules investigate solid films adsorbed onto different substrates, and no previous studies have attempted to cross-reference the study by Campbell *et al* of a $C_{60}$/toluene solution on a mica surface.

## 2. AFM experimental details and results

For our contact-mode AFM measurements, we used a Molecular Imaging Pico SPM with the standard environmental chamber with RHK control electronics and software. The AFM consists of a sharp tip mounted at the end of a compliant cantilever. For these measurements, the tip was held in contact with the sample surface while it was raster scanned across the sample surface. The forces which act on the tip are determined by measuring the angular deflections of the cantilever. These forces both map out the sample surface and measure lateral forces. The MI AFM detects cantilever motion with the standard optical deflection technique [21]. Here, a laser beam is reflected off the back of the cantilever onto the four-quadrant position-sensitive photodiode detector.

Topographic images were acquired by keeping the tip at zero normal load using a feedback system. Overview images were acquired prior to friction measurements to select a smooth, flat area to avoid any topographic contribution to the lateral force. Friction measurements were conducted by raster scanning the tip across the same 100 nm line with the feedback system disabled while varying the normal load. We then plotted lateral force versus normal force for a friction versus load map.

Our measurements were conducted at room temperature and pressure. For measurements acquired under liquid toluene, the AFM cantilever was completely submerged in the liquid to avoid capillary effects, and an open container of toluene was placed inside the environmental chamber to create an air/toluene vapour environment.

The measurements were conducted at low normal loads (smaller than 50 nN). Normal loads were estimated using the normal force constant of the cantilever as specified by the manufacturer (standard oxide-sharpened silicon nitride triangular cantilevers and microprobes from Digital Instruments, 0.58 N $m^{-1}$). Lateral forces are given as voltages ($V$) as measured by the photodiode without further calibration.

The high-purity $C_{60}$ (99.5% $C_{60}$) was purchased from Alfa Aesar in powder form. For the AFM measurements, a solution of toluene and $C_{60}$ was prepared by dissolving 0.1 mg $C_{60}$ for every 1 ml of toluene in order to duplicate the SFA experiment by Campbell and colleagues as closely as possible. The lateral force microscopy (LFM) measurements of mica under toluene and mica under the $C_{60}$/toluene solution were carried out successively with the same cantilever on the same day. A second cantilever was used to acquire the LFM measurements comparing bare mica with mica under toluene.

Atomic-scale AFM images of toluene on mica and the $C_{60}$/toluene solution on mica are shown in figures 1 and 2. As shown in figure 1, AFM atomic-scale images acquired under pure toluene show the periodicity of the mica lattice. For the $C_{60}$ to have an effect on the lateral force, it must form a barrier layer between the AFM tip and the mica. In our measurements, however, the $C_{60}$ did not form the barrier layer, and was instead pushed out of the way by the AFM tip, as is shown in figure 2. For AFM images acquired under the $C_{60}$/toluene solution, the periodicity of the lattice in the image corresponds to the periodicity of the mica lattice. As the spacing between lattice points for $C_{60}$ adsorbed on mica surfaces is double the spacing between lattice points for mica [22], we are certain that our AFM images do not show trapped $C_{60}$ layers.

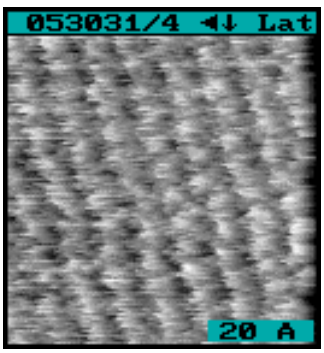


**Figure 1.** An AFM image of mica atoms submerged in toluene.

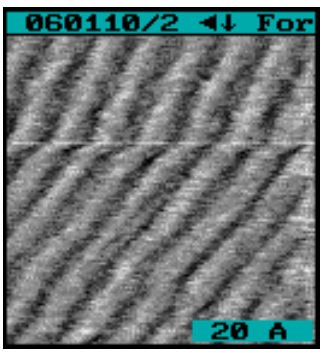


**Figure 2.** An AFM image of mica atoms submerged in the $C_{60}$/toluene solution.

Our results agree with those of Campbell *et al* in the sense that we show that for the slow-moving AFM, the $C_{60}$ monolayers on the mica are easily disrupted, or pushed out of the way. Correspondingly, our measurements of lateral force show no difference between pure toluene on mica and the $C_{60}$/toluene solution on mica, as is shown in figure 3. We do however observe substantially higher friction for bare mica versus mica under toluene (figure 4). This is presumably due to the capillary forces of adsorbed water layers on the AFM tip. For all friction measurements, Amonton's law was obeyed, indicating multi-asperity contacts between the tip and the mica surface.

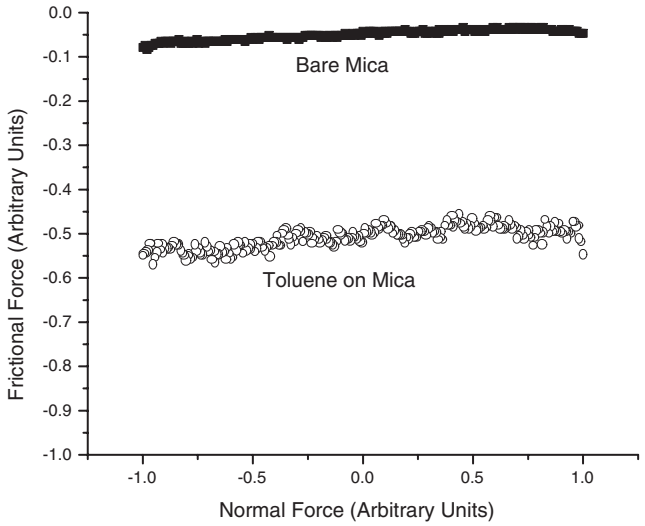


**Figure 3.** Frictional force versus normal force for bare mica and toluene on mica.

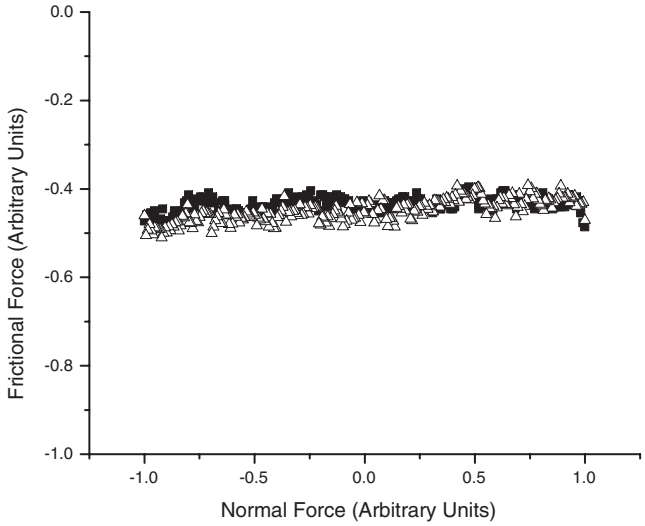


**Figure 4.** Frictional force versus normal force for toluene on mica and $C_{60}$/toluene solution on mica. The two data sets are indistinguishable from one another.

## 3. QCM experimental details and results

### *3.1. The QCM in vacuum*

Our QCM measurements were conducted in ultra-high vacuum (UHV) to avoid monolayers of water and other surface contaminants. The microbalance crystals for these studies were polished 8 MHz AT-cut quartz which had quality factors near $10^5$. The adsorption substrates were silver electrodes deposited on the planar faces of the crystal. We produced the electrodes by evaporation of 99.999% pure Ag at $10^{-8}$ Torr onto the faces of the quartz blanks. During

the desorption process the crystals were radiantly heated by the evaporation boat to temperatures over 200 °C. This procedure produces a mosaic structure with a (111) fibre texture. We then adsorbed toluene onto the Ag(111) surface and monitored both the frequency shift and change in the quality factor with increasing pressure and toluene coverage. Adsorption onto the microbalance produces shifts in both the frequency $f_0$ and the quality factor $Q$, which are indicative of the degree to which the adsorbate is able to track the oscillatory motion of the underlying substrate. Characteristic slip times $\tau$, and friction coefficients (i.e. shear stresses per unit velocity) $\eta$, are determined via the relations [9]

$$\delta(Q^{-1}) = 4\pi\tau\,\delta f_0 \qquad \eta = \frac{\rho_2}{\tau} \tag{3}$$

where $\rho_2$ is the mass per unit area of the adsorbate. In terms of separate phonon and electron–hole slip times [23], $\tau_{ph}$ and $\tau_{eh}$, the slip time $\tau$ can ideally be written as

$$\frac{1}{\tau} = \frac{1}{\tau_{ph}} + \frac{1}{\tau_{eh}}. \tag{4}$$

After measuring the change in frequency and quality factor for toluene on silver, we then again evacuated the chamber to UHV conditions and deposited approximately two monolayers of $C_{60}$ onto the Ag(111). We then again adsorbed toluene onto the $C_{60}$/Ag(111) surface and observed changes in the frequency and quality factor.

Our QCM in UHV results are shown in figure 5 and figure 6. The frequency shift of toluene adsorbed on $C_{60}$/Ag(111) is much larger than that of toluene sliding on Ag(111) (figure 5). The slip time of toluene on Ag(111) is a factor two longer than the slip time of toluene on $C_{60}$/Ag(111) (figure 6). The slip time is proportional to the reciprocal of the coefficient of friction, $\eta$. This means that the friction for toluene sliding on $C_{60}$ is higher than the friction for toluene sliding on Ag(111). We observed only viscous friction, as expected.

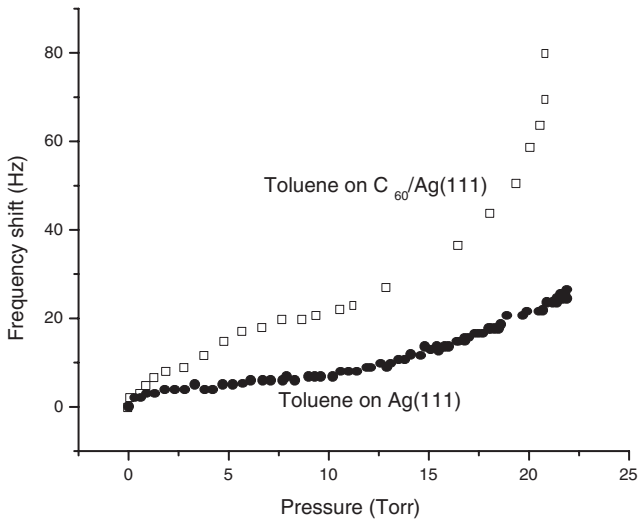


**Figure 5.** QCM frequency shifts for toluene on Ag(111) and toluene on $C_{60}$/Ag(111). The difference between the frequency shift curves for the toluene sliding on $C_{60}$/Ag(111) and the toluene sliding on Ag(111) is due to the wetting [31].

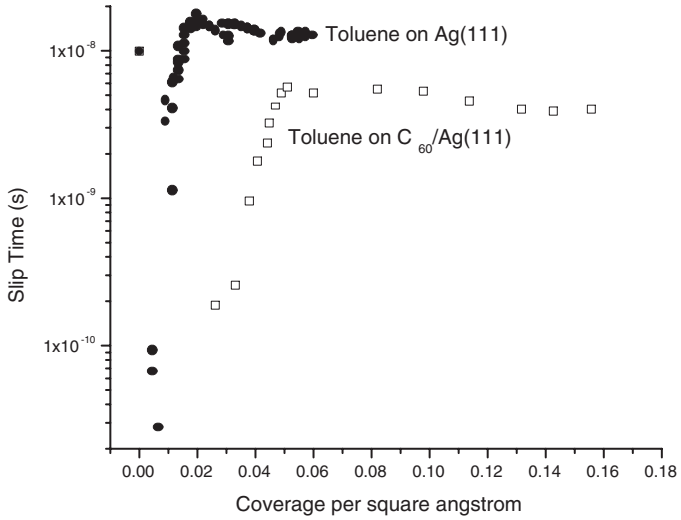


**Figure 6.** QCM slip times for toluene on Ag(111) and toluene on $C_{60}$/Ag(111). The slip time is proportional to the reciprocal of the coefficient of friction, $\eta$. This means that the friction for toluene sliding of $C_{60}$ is approximately twice the friction for toluene sliding on Ag(111).

### *3.2. The QCM in liquids*

The operation of a QCM in a liquid environment has become routine within the last decade [24]. When the electrode operates in contact with a liquid, the shear motion of the surface generates motion in the liquid near the interface. If the surface is sufficiently smooth (as the electrodes on our QCMs are), then the oscillating surface generates plane-parallel laminar flow in the contacting liquid. The response of the oscillator in such conditions depends critically on the viscosity of the fluid adjacent to the electrode, which may well exhibit a structure and viscosity which differs from that of the bulk, and also on whether slippage is occurring at the interface. A variety of models have been developed to predict the oscillator response in a liquid environment, incorporating the possibility of liquid structure and interfacial slip [25–27].

We have made preliminary measurements using a QCM with a gold electrode completely submerged in both pure toluene and the $C_{60}$/toluene solution. We compared the frequency shifts of the QCM between air/toluene and air/solution of $C_{60}$/toluene. The frequency shift of the QCM from air to the solution of $C_{60}$/toluene was a factor two larger than the frequency shift of air/toluene, completely consistent with the QCM in UHV measurements. This suggests that we can correlate bulk, or macroscale, QCM measurements with the monolayer, or nanoscale, measurements acquired in UHV.

## 4. Discussion

Our AFM and LFM results are well correlated with previous SFA results [14]. Although our LFM results do not show a significant change in the lateral force between toluene on mica and the solution of $C_{60}$/toluene on mica as is seen in the SFA, both SFA and AFM results show that the monolayers of $C_{60}$ on mica are easily disrupted.

Our QCM in UHV measures slip times which are due to both the electronic and phononic contributions to friction. For the Ag(111) surface, the atomic surface corrugation is small, which means that the phononic contribution to the friction will be relatively small. The large

number of conduction electrons implies, however, that the electronic contribution to the friction might be relatively large. When monolayers of $C_{60}$ molecules are deposited on the Ag(111) surface, the frictional properties change dramatically. Now, the number of conduction electrons is small, which means that the electronic contribution to the friction will also be small. The surface corrugation, however, is quite large, which causes the phononic contribution to the friction to increase. As we see the friction increase when $C_{60}$ is present, we conclude that phononic friction is dominant for this system.

For our QCM in UHV results, we found that toluene sliding on monolayers of $C_{60}$ deposited onto Ag(111) has a higher friction than that of toluene sliding on Ag(111). The distinguishing feature between our results and previous SFA results is the fact that $C_{60}$ is known to chemisorb onto silver [28, 29] and physisorb onto mica. Therefore the $C_{60}$ molecules are more likely to be mobile on a mica surface than a silver surface. This is confirmed by the fact that we saw no change in the quality factor between the bare Ag(111) surface and the layers of $C_{60}$ on the Ag(111) surface, which indicates that the $C_{60}$ is not slipping on the Ag(111). (Although $C_{60}$ does not slip on the Ag(111) surface, it is known that the $C_{60}$ molecules freely rotate in their lattice position [29].) Our results also show that the full-slip boundary condition found in previous SFA measurements [14] is not due to the slipping of the toluene on the $C_{60}$ molecules. It is more probably due to the slipping of the $C_{60}$ on the mica surface.

## 5. Future work

An ideal cross-referencing experiment would make measurements on the same interface with different techniques, have the same basic geometry throughout and involve simultaneous measurements, ensuring identical conditions. An experiment satisfying these criteria would be a comparison of the QCM with the blow-off technique. The QCM and the blow-off experiment both have open geometries and measure viscous friction. It would also be possible to place the blow-off apparatus atop the QCM, and acquire both QCM and blow-off measurements simultaneously.

Recent theoretical papers [30] have postulated a link between the wetting behaviour of a liquid on a solid and the friction at the solid–liquid interface. In a future experiment, we will test this postulate by comparing contact angle measurements with QCM and AFM measurements of the friction at the interface. It is known that $C_{60}$ chemisorbs onto both copper and silver substrates [28, 29]. However, $C_{60}$ molecules are able to freely rotate in their fixed lattice position on Ag(111), but they are not free to rotate on Cu(111) [29]. We will deposit monolayers of $C_{60}$ onto both Ag(111) and Cu(111) surfaces in UHV, and then measure the contact angle of toluene on $C_{60}$/Ag(111) and $C_{60}$/Cu(111) surfaces. We will then employ the QCM and AFM to measure the friction on these surfaces, and see whether a correlation exists between the wetting behaviour and the friction.

## Acknowledgments

This work was supported by NSF grant No DMR0072030 and AFOSR grant No F49620-98-1-0201 and a Department of Education GAANN Fellowship.

## References

[1] Mate C M and Marchon B 2000 *Phys. Rev. Lett.* **85** 3902
[2] Mate C M, McClelland G M, Erlandsson R and Chang S 1987 *Phys. Rev. Lett.* **59** 1942
[3] Germann G J, Cohen S R, Neubauer G, McClelland G M and Seki H 1993 *J. Appl. Phys.* **73** 163

[4] Israelachvili J N and Tabor D 1973 *Wear* **24** 386
[5] Yoshizawa H, Chen Y L and Israelachvili J N 1993 *J. Phys. Chem.* **97** 4128
[6] Israelachvili J N, McGuiggan P M and Homola A M 1988 *Science* **240** 189
[7] Hirano M, Shinjo K, Kaneko R and Murata Y 1991 *Phys. Rev. Lett.* **67** 2642
[8] Lu C and Czanderna A W (ed) 1984 *Applications of Piezoelectric Quartz Crystal Microbalances* (Amsterdam: Elsevier)
[9] Krim J and Widom A 1986 *Phys. Rev.* B **38** 12 184
[10] Widom A and Krim J 1986 *Phys. Rev.* B **34** R3
[11] Watts E T, Krim J and Widom A 1990 *Phys. Rev.* B **41** 3466
[12] Krim J, Solina D H and Chiarello R 1991 *Phys. Rev. Lett.* **66** 181
[13] Dayo A and Krim J 1998 *Int. J. Thermophys.* **19** 827
[14] Campbell S E, Luengo G, Srdanov V I, Wudl F and Israelachvili J N 1996 *Nature* **382** 520
[15] Bhushan B, Gupta B K, Van Cleef G W, Capp C and Coe J V 1993 *Appl. Phys. Lett.* **62** 3253
[16] Ginzburg B M, Kireenko O F, Baidakova M V and Solovev V A 1999 *Tech. Phys.* **44** 1367
[17] Golan Y, Drummond C, Homyonfer M, Feldman Y, Tenne R and Israelachvili J 1999 *Adv. Mater.* **11** 934
[18] Tochilnikov D G and Ginzburg B M 1999 *Tech. Phys.* **44** 700
[19] Lee S, Shon Y S, Lee T R and Perry S S 2000 *Thin Solid Films* **358** 152
[20] Thundat T, Warmack R J, Ding D and Compton R N 1993 *Appl. Phys. Lett.* **63** 891
[21] Meyer G and Amer N M 1990 *Appl. Phys. Lett.* **57** 2089
[22] Schmicker D, Schmidt S, Skofronick J G, Toennies J P and Vollmer R 1991 *Phys. Rev.* B **44** 10 995
[23] Tomassone M S, Sokoloff J B, Widom A and Krim J 1997 *Phys. Rev. Lett.* **79** 4798
[24] Grate J W, Martin S J and White R M 1993 *Anal. Chem.* **65** 987
[25] Lea M J and Fozooni P 1985 *Ultrasonics* **41** 133
[26] Duncan-Hewitt W C and Thompson M 1992 *Anal. Chem.* **64** 94
[27] Yang M, Thompson M and Duncan-Hewitt W C 1993 *Langmuir* **9** 802
[28] Altman E I and Colton R J 1993 *Surf. Sci.* **295** 13
[29] Sakurai T *et al* 1995 *Appl. Surf. Sci.* **87/88** 405
[30] Barrat J L and Bocquet L 1999 *Phys. Rev. Lett.* **82** 4671
[31] Krim J, Dash J G and Suzanne J 1984 *Phys. Rev. Lett.* **52** 640